Electronic Structure of Cobalt Carbide, CoC

2 AUTHORS:

Demeter Tzeli
National Hellenic Research Foundation
52 PUBLICATIONS **504** CITATIONS

Aristides Mavridis
National and Kapodistrian University of Athens
137 PUBLICATIONS **1,671** CITATIONS

Electronic Structure of Cobalt Carbide, CoC

Demeter Tzeli and Aristides Mavridis*

Laboratory of Physical Chemistry, Department of Chemistry, National and Kapodistrian University of Athens, P.O. Box 64 004, 157 10 Zografou, Athens, Greece

The ground and 18 low lying excited states of the diatomic molecule cobalt carbide, CoC, have been examined by multireference variational methods (MRCI) combined with quantitative basis sets. All calculated states are bound and correlate adiabatically to the ground-state atoms, $Co(a^4F) + C(^3P)$. We report complete potential energy curves, equilibrium bond distances, dissociation energies (D_e), spectroscopic constants, electric dipole moments and spin−orbit splittings. The bonding character of certain states is also discussed with the help of Mulliken distributions and valence-bond-Lewis diagrams. We are practically certain that the ground state is of $^2\Sigma^+$ symmetry with a state of $^2\Delta$ symmetry lying less than 3 kcal/mol higher, in agreement with the relevant experimental findings. Our best estimate of the X $^2\Sigma^+$ dissociation energy is $D_e(D_0) = 83(82)$ kcal/mol at $r_e = 1.541$ Å, 0.02 Å shorter than the experimental bond length.

1. Introduction

The diatomic 3d-transition metal carbides MC, M = Sc−Cu, are clearly of paramount importance for both practical and academic reasons: practical, because M−C bonds are encountered in a plethora of interesting materials, and academic, because the character of the M−C bond does not comply to the conventional "chemical wisdom" about bonding. The reasons for this bonding unorthodoxy have been discussed in our previous publications on ScC,[1a] TiC,[1b] VC,[1c] CrC,[1d] MnC,[1e] and FeC;[1f,g] work in this laboratory is also in progress on NiC and CuC carbides. The vagaries of the 3d-transition metal containing diatomics are described as well in the excellent review article by Harrison.[2]

Henceforth, we present high level multireference variational ab initio calculations on the ground (X) and eighteen (18) excited states (doublets, quartets and sextets) of cobalt carbide, CoC. To the best of our knowledge there are four experimental[3−6] and two theoretical[7,8] studies on CoC.

In 1986, van Zee et al.[3] obtained the ESR spectrum of the CoC radical, and concluded that its lowest state should be of $^2\Sigma$ symmetry. These workers also referred to a $^2\Pi_i$ state interacting strongly with the $^2\Sigma$ and located approximately 66 kcal/mol higher. About 10 years later, Barnes et al.[4] measured the laser-induced fluorescence rotational spectrum of jet-cooled CoC near 750 nm. It was established that the ground state is of $^2\Sigma^+$ symmetry with a low lying $^2\Delta_{5/2}$ state just 221 cm^{-1} higher; its $^2\Delta_{3/2}$ companion is reported to be 1173 cm^{-1} above the X-state, i.e., $\Delta E(^2\Delta_{3/2} \leftarrow {}^2\Delta_{5/2}) = 952$ cm^{-1}. The equilibrium bond lengths and harmonic frequencies of the X $^2\Sigma^+$ and $^2\Delta_{5/2}$ states are $r_0 = 1.5612$, 1.6424 Å and $\omega_e = 934$, 838 cm^{-1}, respectively.[4] They also reported experimental results for three other states ($^2\Sigma^+$, $^2\Pi$, and $\Omega' = 3/2$). Barnes et al. concluded their work by saying: "Various excited states have been observed near 750 nm. Among these are what appears to be a heavily perturbed $^2\Pi_i$ state; its exact nature is unclear and must await detailed ab initio calculations".[4] We will try to shed some light on this $^2\Pi_i$ state, the same one that van Zee and co-workers were referring to 10 years earlier.[3]

In 1997 Adam et Peers[5] through laser-induced fluorescence studies, reported the rotational analysis of the CoC [14.0] $^2\Sigma^+-$X $^2\Sigma^+$ transition. For the X $^2\Sigma^+$ and [14.0]$^2\Sigma^+$ states they obtained $r_0 = 1.5612$ ($r_e = 1.5601$) Å and $r_e = 1.747$ Å, respectively, with $\Delta E([14.0] {}^2\Sigma^+ \leftarrow X {}^2\Sigma^+) = 14243$ cm^{-1} (=40.723 kcal/mol). Adam and Peers close their paper by saying that: "Detailed ab initio calculations on excited states would greatly assist in the further interpretation of these data."[5]

Finally, in 2001, Brewster and Ziurys[6] recorded the pure rotational spectrum of the CoC X $^2\Sigma^+$ state. The equilibrium bond length determined (r_0) was found to be in complete agreement with the results of the previous two optical experimental studies.[4,5]

On the theoretical side now, Gutsev et al.[7] studied the ground states of MC$^{0,\pm}$ carbides (M = Sc−Zn) by density functional theory (DFT); for the entire MC series they report r_e, ω_e, dipole moments (μ), binding energies (D_0), diabatic electron affinities and ionization energies.

Very recently Borin et al.[8] published the first ab initio study on CoC, using the multistate multiconfigurational second-order perturbation theory (MS-CASPT2) of Roos and co-workers,[9] coupled with a newly developed atomic natural orbital basis sets by the same group.[10] These basis sets include scalar relativistic effects obtained through the Douglas−Kroll−Hess (DKH) approach, plus specially tuned functions to account for the $3s^23p^6$ semicore correlation of the metal atom(s). Specifically, the basis set used in this study is $(21s15p10d6f4g2h/_{Co}$ $14s9p4d3f/_C)$ contracted to $[7s6p4d3f2g/_{Co}$ $5s4p3d2f/_C]$. Borin et al.[8] calculated the first seven doublets (X $^2\Sigma^+$, A $^2\Delta$, B $^2\Phi$, C $^2\Phi$, D $^2\Pi$, E $^2\Pi$, [14.0] $^2\Sigma^+$), reporting partial (up to Co−C distances of 2.1 Å) potential energy curves, equilibrium bond lengths, dissociation energies, harmonic frequencies and energy separations. As we will see, their results deviate considerably from the ones obtained here.

In the present work we have performed high level multireference and coupled-cluster (for the two lowest states) calculations in conjunction with large basis sets. For the eight doublets, seven quartets, and four sextets, we report complete

Electronic Structure of Cobalt Carbide

J. Phys. Chem. A, Vol. 110, No. 28, 2006 **8953**

potential energy curves (PEC), energetics, common spectroscopic parameters, and dipole moments; the deciphering of the Co—C bond is also one of the goals of the present study.

In section 2 we define the technical approach followed, in section 3 our results are discussed, and in section 4 some final remarks and comments are presented.

2. Computational Approach

For the Co atom the averaged atomic natural orbital (ANO) basis set of Bauschlicher,[11] (20s15p10d6f4g), and for the C atom the correlation consistent basis set of quadruple cardinality by Dunning,[12] cc-pVQZ = (12s6p3d2f1g) were used. Both sets were generally contracted to [7s6p4d3f2g/$_{Co}$ 5s4p3d2f1g/$_C$], thus containing 139 spherical Gaussian functions. For the two lowest CoC states ($^2\Sigma^+$, $^2\Delta$) the recently developed extended correlation consistent basis sets of quadruple quality by Balabanov and Peterson[13] for the 3d-transition metal elements, cc-pVQZ = 22s18p11d3f2g1h, combined with the cc-pVQZ of Dunning[12] for the C atom were employed, generally contracted to [8s7p5d3f2g1h/$_{Co}$ 5s4p3d2f1g/$_C$] ≡ 4Z. Finally, to account for the $3s^23p^6$ core-valence correlation effects, the cobalt-pVQZ set was augmented by a series of 2s + 2p + 2d + 1f + 1g + 1h weighted core functions, as suggested in ref 13. Combining with the cc-pVQZ basis set of C gives rise to the contracted [10s9p7d4f3g2h/$_{Co}$ 5s4p3d2f1g/$_C$] ≡ C4Z set, spanning a 204 dimensional one-electron space.

The inherent multireference character of CoC and our desire to construct complete potential energy curves (PEC), makes the use of a multireference approach compulsory. Hence, the complete active space self-consistent field + single + double replacements (CASSCF + 1 + 2 = MRCI) methodology was used for all states studied. For the two lowest states ($^2\Sigma^+$, $^2\Delta$) the restricted coupled cluster + singles + doubles + perturbative triples (RCCSD(T)) single reference method was also tried, but using CASSCF natural orbitals.

The multireference zeroth-order functions were built by allocating the 13 active electrons ($3d^74s^2$ on Co + $2s^22p^2$ on C) to a 10 valence orbital space (one 4s and five 3d on Co + one 2s and three 2p on C). The size of our reference spaces range from 474 ($^6\Delta$) to 3526 ($^2\Sigma^+$) configuration functions (CF), with CI spaces ranging from 49×10^6 ($^2\Pi$) to 134×10^6 ($^2\Sigma^+$) CFs. When the internal contraction (icMRCI) scheme of Werner and Knowles is applied,[14] the CI expansions are reduced by about 2 orders of magnitude ($\sim 2.45 \times 10^4$ to 1.22×10^6). The estimation of core-correlation effects (core ≡ $3s^23p^6$ of Co) in the two lowest states was obtained by including the 8 semicore electrons of Co in the CI procedure; these calculations will be referred to as C-MRCI. For the Balabanov–Peterson basis set the C-MRCI (icC-MRCI) expansions contain about 1.7×10^9 (20×10^6) CFs. Scalar relativistic effects for the two lowest $^2\Sigma^+$ and $^2\Delta$ states were estimated through the second-order Douglas–Kroll–Hess[15,16] (DKH2) approximation. For the 1 $^2\Delta$, 2 $^4\Phi$, 3 $^4\Pi$, 4 $^2\Phi$, 5 $^2\Phi$, 6 $^2\Pi$, 7 $^4\Delta$, and 8 $^2\Pi$ states the spin–orbit (SO) splittings were calculated using the previous uncontracted basis sets of Bauschlicher and Dunning (but with the g functions removed) at the MRCI/(20s15p10d6f/$_{Co}$ 12s6p3d2f/$_C$) level of theory through the Breit–Pauli operator.

With the counterpoise technique,[17] the basis set superposition errors (BSSE) of the X $^2\Sigma^+$ and 1 $^2\Delta$ states at the MRCI level were determined to be 0.63 and 0.57 kcal/mol by employing the Bauschlicher (B) basis set on Co.[11] The corresponding values of the Balabanov–Peterson (P) basis (4Z)[13] are 0.65 and 0.60 kcal/mol, respectively.

All calculations were done under C_{2v} symmetry constraints, whereas the CASSCF wave functions were enforced to possess

TABLE 1: Total Energies (hartree) of the $a^4F(4s^23d^7)$ and $b^4F(4s^13d^8)$ States, and the $b^4F \leftarrow a^4F$ Energy Separation (eV) of Co at Different Levels of Theory

	Co		
method[a]	a^4F	b^4F	$b^4F \leftarrow a^4F$
MRCI[b]	−1381.67029	−1381.65300	0.470
MRCI[c]	−1381.67398	−1381.65669	0.471
MRCI+Q[b]	−1381.6886	−1381.6706	0.489
MRCI+Q[c]	−1381.6923	−1381.6740	0.498
MRCI+DKH2[b]	−1392.12073	−1392.09172	0.789
MRCI+DKH2[c]	−1392.11863	−1392.08972	0.787
MRCI+DKH2+Q[b]	−1392.1397	−1392.1102	0.801
MRCI+DKH2+Q[c]	−1392.1373	−1392.1076	0.809
C-MRCI[b]	−1382.00557	−1382.99261	0.353
C-MRCI[c]	−1382.08937	−1382.07717	0.329
C-MRCI+Q[b]	−1382.0503	−1382.0390	0.308
C-MRCI+Q[c]	−1382.1382	−1382.1276	0.284
C-MRCI+DKH2[b]	−1392.51129	−1392.48591	0.691
C-MRCI+DKH2[c]	−1392.53485	−1392.51081	0.654
C-MRCI+DKH2+Q[b]	−1392.5597	−1392.5363	0.638
C-MRCI+DKH2+Q[c]	−1392.5844	−1392.5620	0.609
expt[d]			0.417

[a] Q and DKH2 refer to the Davidson correction and to second-order Douglas–Kroll–Hess scalar relativistic corrections. *[b]* Bauschlicher's basis set for Co, [7s6p4d3f2g]. *[c]* Peterson's basis sets for Co, [8s7p5d3f2g1h] and [10s9p7d4f3g2h] for the C-calculations. *[d]* Reference 21.

axial angular momentum symmetry, i.e., $|\Lambda| = 0$ (Σ), 1 (Π), 2 (Δ) and 3 (Φ). For the excited states 5 $^2\Phi$, 8 $^2\Pi$, 10 $^2\Sigma^+$, 11 $^2\Delta$, 12 $^4\Delta$, 15 $^4\Pi$, and 16 $^4\Phi$ the state average (SA) approach[18] was used due to their strong interaction with states of the same symmetry species.

Finally, it should be mentioned that because of the relatively large number of active electrons (13), the MRCI, and of course more so the C-MRCI calculations, suffer from significant size nonextensivity errors: 11 mh at the MRCI, minimized to about 3 mh after including the Davidson correction[19] for unlinked clusters (+Q) and approximately the same for all studied states.

All calculations were performed with the MOLPRO 2002.6 suite of codes.[20]

3. Results and Discussion

Table 1 records absolute energies of the first two states of the Co atom, $a^4F(4s^23d^7)$ and $b^4F(4s^13d^8)$, along with the $b^4F \leftarrow a^4F$ energy separation at different levels of theory. Observe that at the MRCI level and in both basis sets ((B)auschlicher[11] or (P)eterson[13]), the calculated atomic splitting $b^4F \leftarrow a^4F$ is in fair agreement with the experimental value, 0.470 vs 0.417 eV.[21] However, by increasing the sophistication of the method from MRCI to C-MRCI + DKH2 + Q, the theoretical results depart monotonically from the experimental value. Obviously, the good MRCI agreement is rather fortuitous due to cancellation of errors.

The ground states of Co(a^4F) and C(^3P) give rise to a total of 36 molecular CoC $^{2S+1}\Lambda$ states, namely, $^{2S+1}$(Γ[1], Φ[2], Δ[3], Π[3], Σ[3]) with $2S + 1 = 2$, 4, and 6, out of which the first nineteen have been investigated as indicated by preliminary CASSCF calculations.

Numerical results of the first two lower states $^2\Sigma^+$ and $^2\Delta$ in a variety of methods, and of the remaining seventeen states limited to the MRCI or MRCI+Q/[7s6p4d3f2g/$_{Co}$ 5s4p3d2f1g/$_C$] level, are listed in Table 2. For all 19 states Table 3 catalogues leading MRCI configurations and atomic Mulliken populations, valence-bond-Lewis (vbL) diagrams indicating graphically the bonding character of every state, and asymptotic fragments. Figure 1 depicts a relative level diagram of the states studied

TABLE 2: Absolute Energies E (hartree), Bond Lengths r_e (Å), Binding Energies D_e (kcal/mol), Harmonic Frequencies and Anharmonic Corrections ω_e, $\omega_e x_e$ (cm^{-1}), Rotational Vibrational Couplings α_e (cm^{-1}), Centrifugal Distortions $\bar{D}_e$ (cm^{-1}), Total Mulliken Charges on Co q_{Co}, Dipole Moments μ (Debye), and Energy Differences T_e (kcal/mol), at Various Levels of Theory (Experimental and Other Theoretical Results Also Included)

state	methods[a]	−E	r_e	D_e	ω_e	$\omega_e x_e$	$10^{-3}\alpha_e$	$10^{-7}\bar{D}_e$	q_{Co}	$\langle\mu\rangle$[b]	μ_{FF}[b]	T_e
X $^2\Sigma^{+}$ [c]	CASSCF	1419.18907	1.569	41.0	887.1	10.56	7.72	1.65	0.10	1.00	1.00	0.0
		(1419.18986)	(1.569)	(41.2)	(886.4)	(10.5)	(7.77)	(1.65)	(0.24)	(0.94)	(0.94)	(0.0)
	MRCI	1419.57221	1.548	80.4	965.4	5.66	5.71	1.51	0.06	0.86	1.82	0.0
		(1419.57619)	(1.547)	(80.7)	(967.0)	(5.56)	(5.69)	(1.51)	(0.17)	(0.80)	(1.81)	(0.0)
	MRCI+Q	1419.6075	1.552	84.2								2.07	0.0
		(1419.6112)	(1.550)	(84.3)								(2.07)	(0.0)
	MRCI+DKH2	1430.03368	1.542	77.9	982.1	6.04	5.90	1.49	0.21	0.94	1.86	0.0
		(1430.03097)	(1.542)	(77.7)	(979.9)	(5.79)	(5.88)	(1.50)	(0.18)	(0.94)	(1.87)	(0.0)
	MRCI+DKH2+Q	1430.06974	1.545	81.7								2.09	0.0
		(1430.0664)	(1.545)	(81.3)								(2.08)	(0.0)
	C-MRCI[d]	1419.90261	1.544	82.3	984.0	5.16	5.46	1.47	0.06	0.80	1.76	0.0
		(1419.98210)	(1.544)	(80.5)	(980.2)	(3.90)	(5.29)	(1.49)	(0.32)	(0.73)	(1.72)	(0.0)
	C-MRCI+Q[d]	1419.97302	1.546	88.7								2.06	0.0
		(1420.0573)	(1.546)	(86.9)								(2.03)	(0.0)
	C-MRCI+DKH2[d]	1430.41435	1.541	77.1	993.8	5.76	5.60	1.46	0.23	0.90	1.81	0.0
		(1430.43747)	(1.540)	(77.4)	(993.4)	(5.26)	(5.55)	(1.47)	(0.33)	(0.89)	(1.79)	(0.0)
	C-MRCI+DKH2+Q[d]	1430.4888	1.542	83.5								2.08	0.0
		(1430.5132)	(1.541)	(83.8)								(2.07)	(0.0)
	RCCSD(T)	1419.61621	1.541	84.0	1004	6.9					2.05	0.0
	RCCSD(T)+DKH2	1430.07947	1.534	81.6	1018	9.8					2.04	0.0
	C−RCCSD(T)[d]	1419.99942	1.537	87.7	1032						2.10	0.0
	C−RCCSD(T)+DKH2[d]	1430.51990	1.532	82.5									0.0
	DFT/BPW91[e]		1.542	107	1050							2.16	0.0
	DFT/BLYP[e]		1.552	106	1027							2.14	0.0
	DFT/B3LYP[e]		1.527	72.7	700							2.35	0.0
	CASPT2+DKH[f]	1430.0473[g]	1.579	110.7	868				0.39				
	expt		1.5612[h,i,j]		934[h]							
	expt		1.5601[i]									
1 $^2\Delta$ [c]	CASSCF	1419.19588	1.674	45.3	735.0	13.54	8.53	1.63	0.20	2.02	2.02	−4.27
		(1419.19653)	(1.674)	(45.4)	(735.1)	(13.54)	(8.52)	(1.63)	(0.32)	(2.04)	(2.04)	(−4.18)
	MRCI	1419.56963	1.656	78.7	821.2	2.86	5.45	1.39	0.15	1.72	2.08	1.62
		(1419.57360)	(1.654)	(78.9)	(824.4)	(4.06)	(5.23)	(1.39)	(0.24)	(1.73)	(2.10)	(1.62)
	MRCI+Q	1419.6070	1.656	83.7								1.90	0.33
		(1419.6109)	(1.654)	(83.9)								(1.92)	(0.2)
	MRCI+DKH2	1430.03679	1.638	79.7	848.3	5.74	5.73	1.39	0.22	1.66	2.03	−1.95
		(1430.03404)	(1.640)	(79.5)	(847.3)	(5.77)	(5.69)	(1.39)	(0.23)	(1.67)	(2.03)	(−1.92)
	MRCI+DKH2+Q	1430.0749	1.640	84.8								1.87	−3.27
		(1430.0717)	(1.640)	(84.5)								(1.87)	(−3.3)
	C-MRCI[d]	1419.89795	1.653	79.4	837.5	2.51	4.85	1.35	0.17	1.76	2.16	2.92
		(1419.97711)	(1.654)	(77.2)	(833.8)	(2.18)	(4.78)	(1.36)	(0.38)	(1.79)	(2.20)	(3.12)
	C-MRCI+Q[d]	1419.9701	1.650	86.9								2.06	1.83
		(1420.0542)	(1.652)	(84.8)								(2.13)	(1.9)
	C-MRCI+DKH2[d]	1430.41571	1.639	77.9	852.3	4.73	5.17	1.37	0.24	1.72	2.12	−0.86
		(1430.43810)	(1.640)	(77.6)	(851.3)	(4.39)	(5.34)	(1.37)	(0.37)	(1.72)	(2.15)	(−0.39)
	C-MRCI+DKH2+Q[d]	1430.4920	1.638	85.3								2.04	−2.01
		(1430.5156)	(1.638)	(85.1)								(2.08)	(−1.6)
	RCCSD(T)	1419.61577	1.646	83.7	888						1.47	0.28
	UCCSD(T)	1419.61724	1.649	84.4	891	2.4					1.49	−0.37
	C−UCCSD(T)[d]	1419.99923	1.638	87.2	908						1.47	0.49
	CASPT2+DKH[f]		1.637	112.5	1078							−1.72
	expt[h]		1.6424		838							1.993
2 $^4\Phi$	CASSCF	1419.17200	1.976	31.0	458.4	12.92	−2.98	1.56	0.45	2.63	2.63	10.7
	MRCI	1419.54220	1.641	62.0	863.0	3.11	3.99	1.33	0.23	2.00	2.82	18.8
	MRCI+Q	1419.5798	1.630	67.2								2.93	17.4
3 $^4\Pi$	CASSCF	1419.16442	2.000	26.7	456.2	11.37	−1.54	1.46	0.45	2.78	2.78	15.5
	MRCI	1419.54014	1.634	60.5	863.4	5.71	3.32	1.36	0.22	2.03	2.83	20.1
	MRCI+Q	1419.5786	1.627	66.0								2.94	18.2
4 $^2\Phi$	CASSCF	1419.17615	1.967	33.6	502.0	3.59	1.62	1.33	0.44	2.66	2.66	8.11
	MRCI	1419.53093	1.713	54.9	598.2	12.10	11.73	2.14	0.28	1.67	2.24	25.9
	MRCI+Q	1419.5654	1.682	58.1								2.29	26.5
	CASPT2+DKH[f]		1.632	85.3	993							25.47
5 $^2\Phi$	MRCI	1419.52222	1.657	50.3	837.6	5.21	4.60	1.33	0.20	1.59	2.36	31.4
	MRCI+Q	1419.5590	1.652	54.5								2.45	30.5
	CASPT2+DKH[f]		1.622	81.2	1159							29.54
6 $^2\Pi$	CASSCF	1419.16755	2.002	28.7	501.9	3.49	2.68	1.19	0.45	2.86	2.86	13.5
	MRCI	1419.51843	1.745	46.9	403	20.1	1.81	3.47	0.30	1.81	2.34	33.7
	MRCI+Q	1419.5534	1.677	50.2								2.27	34.0
	CASPT2+DKH[f]		1.622	80.3	1105							30.48
$^2\Pi_{3/2}$	expt[h]		1.6439										37.39
$^2\Pi_{1/2}$	expt[h]		1.7204										38.15
7 $^4\Delta$	CASSCF	1419.16946	1.989	28.7	508.9	3.84	2.93	1.21	0.42	2.39	2.39	12.3
	MRCI	1419.51747	1.829	46.0	465	17			0.29	1.35	1.68	34.3
	MRCI+Q	1419.5504	1.795	48.2								1.36	35.9

Electronic Structure of Cobalt Carbide

J. Phys. Chem. A, Vol. 110, No. 28, 2006 **8955**

TABLE 2: (Continued)

state	methods[a]	−E	r_e	D_e	ω_e	$\omega_e x_e$	$10^{-3}\alpha_e$	$10^{-7}\bar{D}_e$	q_{Co}	$\langle\mu\rangle$[b]	μ_{FF}[b]	T_e
8²Π	MRCI	1419.51524	1.665	45.8	1130.7	49.4	3.95	0.718	0.20	1.59	2.61	35.7
	MRCI+Q	1419.5540	1.655	51.3							2.74	33.6
	CASPT2+DKH[f]		1.642	75.4	949							35.41
9 ⁴Σ⁺	CASSCF	1419.16316	2.046	24.7	501.1	4.05	2.72	1.05	0.48	3.03	3.03	16.3
	MRCI	1419.50573	1.755	38.7	451	63			0.32	1.58	2.18	41.7
	MRCI+Q	1419.5401	1.698	41.9							2.67	42.3
10 ²Σ⁺	MRCI	1419.50064	1.764	36.7	721	2.8			0.22	1.40	2.34	44.9
	MRCI+Q	1419.5385	1.745	41.6							2.44	43.3
	CASPT2+DKH[f]		1.676	73.1	1252							37.67
	expt[h]		~1.80		685							39.89
	expt[i]		1.747		617		5.31					40.72
11 ²Δ	MRCI	1419.49971	1.726	36.2	716				0.17	0.082	0.68	45.5
	MRCI+Q	1419.5349	1.709	39.4							0.81	45.6
Ω′ = ³/₂	expt[h]		1.75		643							38.39
12 ⁴Δ	MRCI	1419.49962	1.776	36.0	904.0	13.0	4.36	7.56	0.24	1.19	1.67	45.6
	MRCI+Q	1419.5349	1.763	39.4							1.63	45.5
13 ⁶Φ	CASSCF	1419.16320	2.048	25.4	525.0	3.44	3.12	9.50	0.47	2.68	2.68	16.2
	MRCI	1419.49911	1.953	35.0	496.4	3.29	2.10	1.41	0.40	2.15	2.23	45.9
	MRCI+Q	1419.5284	1.933	34.9							2.59	49.7
14 ⁶Σ⁺_G[k]	CASSCF	1419.15865	2.064	21.9	515.6	4.10	3.34	9.40	0.48	2.95	2.95	19.1
	MRCI	1419.49496	1.975	31.9	473.5	9.97	−1.05	1.46	0.41	2.55	3.06	48.5
	MRCI+Q	1419.5246	1.954	32.1							3.08	52.0
14 ⁶Σ⁺_L[k]	MRCI	1419.49301	1.694	30.7	979	10.4			0.34	2.58	3.85	49.7
	MRCI+Q	1419.5290	1.676	34.9							3.92	49.3
15 ⁴Π	MRCI	1419.49391	1.780	32.4	824.0	13.2	7.32	8.80	0.26	1.86	3.00	49.1
	MRCI+Q	1419.5306	1.760	36.6							3.00	48.3
16 ⁴Φ	MRCI	1419.49353	1.826	32.3	767.4	18.8	3.49	8.87	0.28	1.89	2.81	49.4
	MRCI+Q	1419.5276	1.809	34.9							2.92	50.2
17 ⁶Π	CASSCF	1419.15650	2.067	21.7	507.8	3.66	3.23	0.962	0.47	2.82	2.82	20.4
	MRCI	1419.49249	1.987	31.1	483.5	3.09	2.18	1.35	0.40	2.36	2.72	50.0
	MRCI+Q	1419.5220	1.975	31.0							2.68	53.7
18 ⁶Δ	CASSCF	1419.15730	2.073	21.1	497.6	3.37	3.26	0.983	0.47	2.64	2.64	19.9
	MRCI	1419.49127	2.003	29.5	477.0	2.36	3.07	1.31	0.40	2.15	2.39	50.8
	MRCI+Q	1419.5203	1.997	29.4							2.32	54.7

[a] Q and DKH2 refer to Davidson and to second-order Douglas−Kroll−Hess relativistic corrections. [b] $\langle\mu\rangle$ calculated as expectation value, μ_{FF} by the finite field method. [c] Numbers in parentheses are calculated using the Peterson's basis set cc-pVQZ. [d] Semicore $3s^23p^6$ electrons of the Co atom included in the CI. [e] Reference 7. [f] Reference 8. [g] The energy value is estimated from Figure 1 of ref 8. [h] Reference 4, r_0 value. [i] Reference 5. [j] Reference 6, r_0 value. [k] G and L refer to global and local minima.
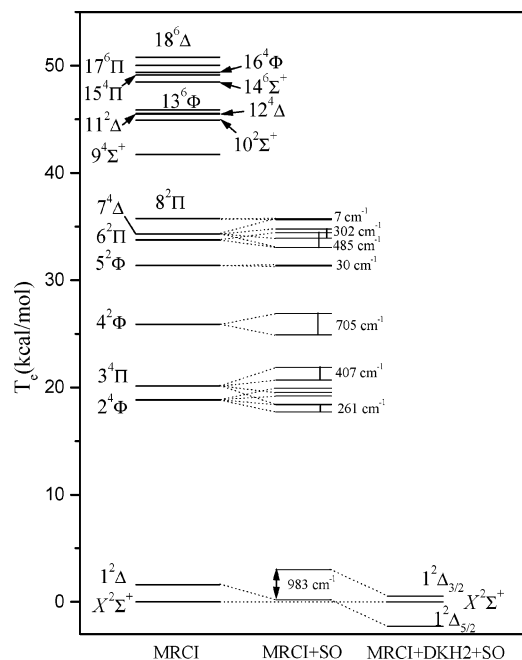
Figure 1. MRCI relative energy levels of CoC including SO splittings.

Figure 2. Potential energy curves of 19 states of CoC at the MRCI/[7s6p4d3f2g/_Co 5s4p3d2f1g/_C] level of theory.

along with SO-splittings of the 1 ²Δ, 2 ⁴Φ, 3 ⁴Π, 4 ²Φ, 5 ²Φ, 6 ²Π, 7 ⁴Δ, and 8 ²Π states, and Figure 2 displays the totality of PECs studied. Each excited state has been labeled with a serial number in front of the symmetry symbol revealing its absolute energy order with respect to the ground (X) state.

Finally, Figures 3−5 present separately the PECs according to their spin multiplicity. Note that all states correlate to the ground-state atoms, Co(a⁴F) + C(³P).
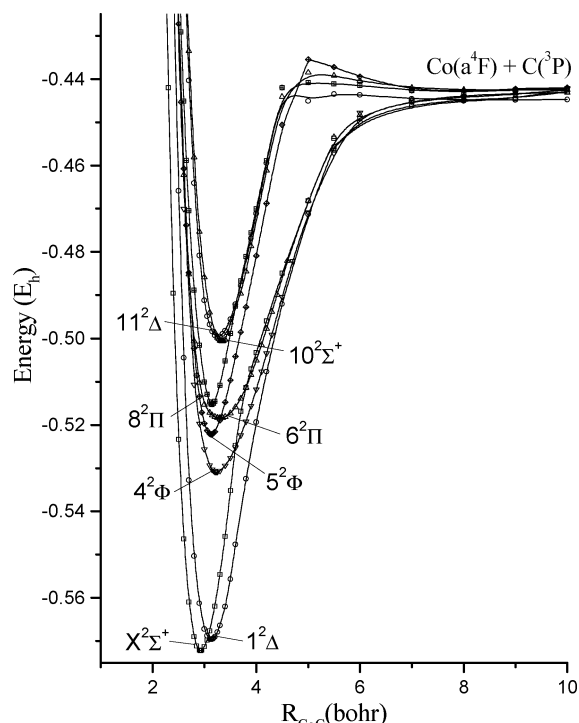
Figure 3. MRCI potential energy curves of the CoC doublets.

Figure 5. MRCI potential energy curves of the CoC sextets.

Figure 4. MRCI potential energy curves of the CoC quartets.

In what follows we examine first the doublets, then the quartets and finally the sextets.

A. Doublets: $X^2\Sigma^+$, $1^2\Delta$, $4^2\Phi$, $5^2\Phi$, $6^2\Pi$, $8^2\Pi$, $10^2\Sigma^+$, and $11^2\Delta$. Experimentally, the ground state of CoC is of $^2\Sigma^+$ symmetry,[3-6] and the same could be said theoretically but not without some reservations (see below). According to Table 3 the asymptotic wave function can be described by the product $|a^4F; M = 0\rangle_{Co} \times |^3P; M = 0\rangle_C$. As the two atoms come closer, an avoided crossing occurs around 3.8 bohr with the $10\ ^2\Sigma^+$ state. However, the latter had already suffered an avoided crossing with an incoming (not calculated) $^2\Sigma^+$ state correlating

to the b^4F state of the Co atom. As a result, the equilibrium atomic character of the $X^2\Sigma^+$ is Co(b^4F, s^1d^8; $M = 0$) + C(^3P; $M = 0$). The atomic Mulliken populations and the leading configuration point clearly to a triple $2\pi + \sigma$ bond between the Co and C atoms, as shown in the vbL diagram of Table 3. About 0.5 e^- are transferred from the $\sim4p3d_{z^2}$ Co hybrid to the empty $2p_z$ orbital of the C atom ($M = 0$), with 0.4 e^- leaking back to the metal through the π_x, π_y system.

Table 2 lists total energies, spectroscopic parameters and dipole moments of the $X\ ^2\Sigma^+$ and $1\ ^2\Delta$ states obtained at the multireference and coupled-cluster methods. Notice that at the MRCI, MRCI+Q, MRCI+DKH2, and MRCI+DKH2+Q levels of theory, all our results are almost identical in both B and P basis sets. Moving to C-level, i.e., including the $3s^23p^6$ electrons of Co in the CI procedure, only slight differences are observed between the B and P bases in all properties studied. At the highest level of theory, namely, C-MRCI+DKH2+Q+BSSE/ C4Z, $D_e(D_0) = 83(82)$ kcal/mol with respect to the ground-state atoms, and $r_e = 1.541$ Å, 0.02 Å shorter than the experimental one.[4-6] It is interesting that exactly the same D_e value is obtained at the "simple" valence MRCI+Q and RCCSD(T) levels with $r_e = 1.550$ and 1.541 Å, respectively. We recall that the D_e values of all triple bonded MC carbides, that is VC($X\ ^2\Delta$),[1c] CrC($X\ ^3\Sigma^-$),[1d] MnC($X\ ^4\Sigma^-$),[1e] FeC($X\ ^3\Delta$),[1f,g] and NiC($X\ ^1\Sigma^+$)[22] obtained at about the same level of theory as the present one, are 95, 89, 70, 90, and 87 kcal/mol, respectively, in conformity with the D_e value of the $X\ ^2\Sigma^+$ state of CoC. Corresponding experimental results for the ground states of VC,[23] FeC,[24] and NiC[25] are 100.1 ± 5.7, 91.2 ± 7, and larger than 78.2 kcal/mol, respectively; no experimental results are available for the CrC and MnC carbides. Hence, we believe that the reported dissociation energy of $D_e = 111$ kcal/mol by Borin et al.,[8] is rather overestimated by about 25−30 kcal/mol.

The next state is of $^2\Delta$ symmetry, correlates to Co(a^4F; $M = \pm2$) + C(^3P; $M = 0$), and suffers an avoided crossing around 4 bohr with the $11\ ^2\Delta$ state. Thus its in situ equilibrium atoms switch to Co(a^4F; $M = \pm3$) + C(^3P; $M = \mp1$), and it is

Electronic Structure of Cobalt Carbide

J. Phys. Chem. A, Vol. 110, No. 28, 2006 **8957**

genuinely triple bonded with a slightly negative carbon atom ($\sim$0.2 e$^-$). Although we have tagged the ground state as $^2\Sigma^+$ following the experimentalists, our calculations indicate that a $^2\Delta$ symmetry is a strong contender for being the lowest state; it is interesting to follow the results of Table 2. At the valence MRCI(+Q) level, $T_e(^2\Delta\leftarrow^2\Sigma^+) = 1.62(0.2)$ kcal/mol, but the picture changes by adding the scalar relativistic effects, namely, $T_e(^2\Delta\leftarrow^2\Sigma^+) = -1.92(-3.3)$ kcal/mol, the $^2\Delta$ state becoming now the lowest. At the C-MRCI(+Q)/C4Z level, $T_e(^2\Delta\leftarrow^2\Sigma^+) = 3.12(1.9)$ kcal/mol. However, at the highest level of calculation, C-MRCI+DKH2(+Q)/C4Z, $T_e = -0.39(-1.6)$ kcal/mol, i.e., the $^2\Delta$ state is lower than the $^2\Sigma^+$ by about 1.6 kcal/mol.

Experimentally, the $^2\Delta_{5/2}$ and $^2\Delta_{3/2}$ states are 221 and 1173 cm^{-1} above the $^2\Sigma^+$ state,[4] with the mean value 697 cm^{-1} (=1.99 kcal/mol) higher. This number is in excellent agreement with the valence MRCI and C-MRCI+Q/C4Z results of the present work, which predict that $T_e(^2\Delta\leftarrow^2\Sigma^+) = 1.62$ and 1.9 kcal/mol, respectively; it is the addition of the scalar relativistic effects that inverts the two states, suggesting that the $^2\Delta$ is lower by 1.6 kcal/mol with respect to $^2\Sigma^+$. Recall, however, that the $^2\Sigma^+$ state correlates *diabatically* to the first excited b^{4}F(4s^{1}3d^8) state of Co, whereas the $^2\Delta$ to the a^{4}F(4s^{2}3d^7). The C-MRCI+DKH2+Q/C4Z b^{4}F $\leftarrow$ a^{4}F energy separation is 0.609 eV (Table 1), 0.192 eV *higher* than the experimental one, and this large error is the cause of predicting the $^2\Delta$ state lower than the $^2\Sigma^+$ at this level of theory. By parallel downshifting of the $^2\Sigma^+$ PEC by 0.192 eV = 4.43 kcal/mol, the $^2\Sigma^+$ becomes the ground state, lying approximately 4.4$-$1.6 = 2.8 kcal/mol lower than the $^2\Delta$, and in fair agreement now with experiment. Therefore, it seems rather certain that the ground state of CoC is of $^2\Sigma^+$ symmetry.

Finally, we report that the MRCI/(20s15p10d6f/$_{Co}$ 12s6p3d2f/$_C$) $^2\Delta_{3/2} - {}^2\Delta_{5/2}$ SO-splitting is calculated to be 989 cm^{-1}, in rather good agreement with the experimental[4] value of 952 cm^{-1}.

The next two doublets $4^2\Phi$ and $5^2\Phi$ are of intense multireference character; they are double bonded (σ, π) and correlate to Co(a^{4}F; $M = \pm3, \pm2$) + C(^{3}P; $M = 0, \pm1$), respectively (Table 3). An avoided crossing at 5.0 bohr of $5^2\Phi$ with another (not calculated) $^2\Phi$ state correlating to the b^{4}F atomic state of Co, transforms its character to Co(b^{4}F; $M = \pm3$) + C(^{3}P; $M = 0$); the strong interaction of the $5^2\Phi$ and $4^2\Phi$ states, which follows around equilibrium ($\sim$3 bohr), increases the complexity of these two $^2\Phi$ states.

Their MRCI(+Q) D_e and r_e values are 54.9(58.1), 50.3(54.5) kcal/mol and 1.713(1.682), 1.657(1.652) Å, respectively. The MRCI/(20s15p10d6f/$_{Co}$ 12s6p3d2f/$_C$) SO splittings of $4^2\Phi$ and $5^2\Phi$ states are $\Delta E(^2\Phi_{7/2}-{}^2\Phi_{5/2}) = 705$ and 30 cm^{-1}, respectively; Figure 1. The results of Borin et al.[8] differ significantly from ours, most notably in the dissociation energies. It is curious that the D_e values of all seven doublets calculated in ref 8 are systematically larger than the corresponding ones calculated presently by about 30 kcal/mol; see Table 2.

Two $^2\Pi$ states, almost degenerate, marked $6\ ^2\Pi$ and $8\ ^2\Pi$, have been obtained at the MRCI(+Q) level of theory with energy distances from the X $^2\Sigma^+$ state of 33.7(34.0) and 35.7(33.6) kcal/mol, respectively. Both are of intense multireference nature, double bonded (σ, π) and correlating to Co(a^{4}F; $M = \pm1, \pm2$) + C(^{3}P; $M = 0, 1$). The $8\ ^2\Pi$ suffers two avoided crossings around 6.5 and 5.0 bohr with a higher (not calculated) $^2\Pi$ state. Passing the equilibrium of the $6\ ^2\Pi$ state, $r_e = 1.745$ Å (=3.30 bohr), the $8\ ^2\Pi$ suffers a third avoided crossing now with the $6\ ^2\Pi$ state, very close to its equilibrium geometry, $r_e = 3.13$ bohr. The MRCI SO splittings of the 6 and 8 $^2\Pi$ states, are $\Delta E(^2\Pi_{3/2} - {}^2\Pi_{1/2}) = 485$ and 7 cm^{-1}, respectively; Figure 1. Experimentally,[4] two transitions at 13343 and 13079 cm^{-1}

have been observed, which probably correspond to the $v = 0$ SO components of the $^2\Pi_i$ state, with $\Delta E(^2\Pi_{3/2} - {}^2\Pi_{1/2}) = 264$ cm^{-1}. Because the 6 and 8 $^2\Pi$ states are practically degenerate at the MRCI+Q level, we cannot tell with certainty to which one the experimentally determined $^2\Pi_i$ state corresponds. Perhaps, the two X$-^2\Pi_i$ transitions that the experimentalists see are not the 3/2 and 1/2 components of one $^2\Pi$ state, but belong to the two $^2\Pi$ degenerate states, i.e., (8 $^2\Pi_{1/2,3/2}$, 6 $^2\Pi_{1/2}$) $\leftarrow$ X $^2\Sigma^+$.

10 $^2\Sigma^+$. This is a triple bonded strongly multireference state correlating to Co(a^{4}F; $M = \pm1$) + C(^{3}P; $M = \mp1$); see Table 3. There are two avoided crossings, one at 5 bohr with the higher excited state $^2\Sigma^+$ correlating to Co(b^{4}F; $M = 0$) + C(^{3}P; $M = 0$), and then at 3.8 bohr with the ground state. As a result, the in situ equilibrium atoms are Co(a^{4}F; $M = 0$) + C(^{3}P; $M = 0$). Experimentally, the 10 $^2\Sigma^+$ state is located 39.89[4] or 40.72 kcal/mol[5] (T_e) above the X state, with an r_e of 1.747 Å.[5] Our MRCI(+Q) results are in acceptable agreement with these experimental findings, namely, $T_e = 44.9(43.3)$ kcal/mol and $r_e = 1.764(1.745)$ Å; Table 2.

11 $^2\Delta$. This is the highest of the doublets studied, double bonded (π, π), with $D_e = 36.2(39.4)$ kcal/mol, $T_e = 45.5(45.6)$ kcal/mol, and $r_e = 1.726$ (1.709) Å at the MRCI(+Q) level; see Tables 2 and 3. Experimentally, a state at $T_0 = 38.39$ kcal/mol[4] and $r_0 = 1.75$ Å with a total angular momentum $\Omega' = {}^3/_2$ has been observed, which could be the 3/2 component of either a $^2\Pi$ or $^2\Delta$ state.

B. Quartets: 2 $^4\Phi$, 3 $^4\Pi$, 7 $^4\Delta$, 9 $^4\Sigma^+$, 12 $^4\Delta$, 15 $^4\Pi$, and 16 $^4\Phi$. The potential energy curves of the seven quartets studied in the present work are displayed in Figure 4; the MRCI/(20s15p10d6f/$_{Co}$ 12s6p3d2f/$_C$) SO-splittings of the 2 $^4\Phi$, 3 $^4\Pi$, and 7 $^4\Delta$ states are shown in Figure 1.

2 $^4\Phi$, 16 $^4\Phi$. Formally, the 2 $^4\Phi$ is the lowest of the quartets with a $^4\Pi$ state just 1.3(0.8) kcal/mol higher at the "simple" MRCI(+Q) level. Whereas both $^4\Phi$ correlate to the ground-state atoms Co(a^{4}F; 4s^{2}3d^7) + C(^{3}P), the 16 $^4\Phi$ experiences an avoided crossing around 4.6 bohr with a higher (not calculated) $^4\Phi$ correlating to the first excited state of Co(b^{4}F; 4s^{1}3d^8) + C(^{3}P). As we move closer to equilibrium, it seems that the 16$^4\Phi$ state interacts with the 2 $^4\Phi$ at about 3.5 bohr; therefore, the in situ equilibrium character of Co atom in the latter acquires the 4s^{1}3d^8 distribution. The resulting double bond (σ, π) character in the 2 $^4\Phi$ state of CoC, along with Mulliken populations and leading configurations, are depicted in Table 3. The bonding in the 16 $^4\Phi$ state is also (σ, π), but now the in situ Co atom possesses a 4s^{2}3d^7(a^{4}F) distribution; see the vbL diagram in Table 3. At the MRCI(+Q) level the 2 $^4\Phi$ and 16 $^4\Phi$ states are located 18.8(17.4) and 49.4(50.2) kcal/mol above the X state with binding energies with respect to Co(a^{4}F) + C(^{3}P) of, $D_e = 62.0(67.2)$ and 32.3(34.9) kcal/mol, respectively (Table 2).

3 $^4\Pi$, 15 $^4\Pi$. Recall that under C_{2v} symmetry the Π and Φ states have the same spatial symmetry, i.e., B$_1$. The 3 $^4\Pi$ is practically degenerate to 2 $^4\Phi$, and the 15 $^4\Pi$ to 16 $^4\Phi$. In all respects these two $^4\Pi$ states are strikingly similar to the two $^4\Phi$ states just discussed; see Tables 2 and 3.

7 $^4\Delta$, 12 $^4\Delta$. Both these quartets are double bonded, of (σ, π) character the 7 $^4\Delta$ and (π, π) the 12 $^4\Delta$ state; see Table 3. The 12 $^4\Delta$ suffers an avoided crossing around 4.5 bohr with an incoming (not calculated) $^4\Delta$ state correlating to Co(b^{4}F; 4s^{1}3d^8) + C(^{3}P), therefore imparting this character to the in situ equilibrium atoms of the 12 $^4\Delta$ state. An avoided crossing also occurs between the 7 $^4\Delta$ and 12 $^4\Delta$ states in the repulsive part of their potential energy curves (Figure 4).

TABLE 3: MRCI Leading Configurations, Mulliken Populations, Valence-Bond-Lewis Diagrams and M(Co), M(C) Projection Values of Asymptotic Atoms, Co(a⁴F; M) + C(³P; M)
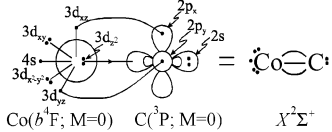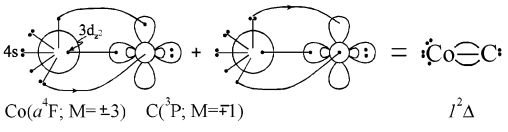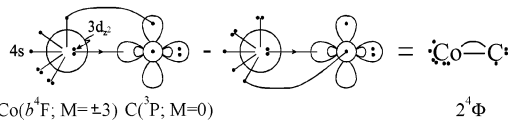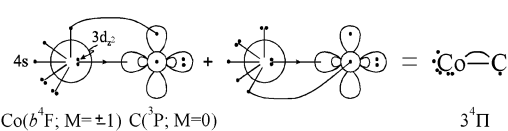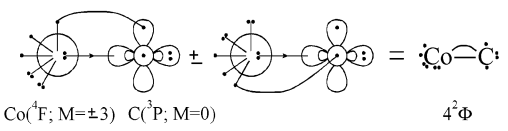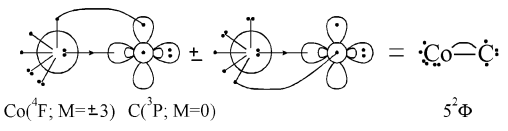
State	Leading Configurations	Population Analysis	vbL	M, M
$X^2\Sigma^+$	$0.85\left\|1\sigma^2 2\sigma^2 3\sigma^1 1\pi_x^2 1\pi_y^2 1\delta_+^2 1\delta_-^2\right\rangle_{A_1}$	$4s^{0.92}4p_z^{0.21}3d_{z^2}^{1.36}3d_{xz}^{1.22}4p_x^{0.03}3d_{yz}^{1.22}4p_y^{0.03}3d_{x^2-y^2}^{1.97}3d_{xy}^{1.97}$ $2s^{1.73}2p_z^{0.75}2p_x^{0.75}2p_y^{0.75}$	Co(b^4F; M=0) C(^{3}P; M=0) $X^2\Sigma^+$	0, 0
$1^2\Delta$	$\frac{1}{\sqrt{2}}\left\|1\sigma^2 2\sigma^2 3\sigma^2\left[0.81\left(1\pi_x^2 1\pi_y^2\right)-0.18\left(1\pi_x^2 2\pi_y^2 + 2\pi_x^2 1\pi_y^2\right)\right]\times\left(1\delta_+^2 1\delta_-^1 + 1\delta_+^1 1\delta_-^2\right)\right\rangle_{A_1+A_2}$	$4s^{1.24}4p_z^{0.16}3d_{z^2}^{1.64}3d_{xz}^{1.36}4p_x^{0.04}3d_{yz}^{1.36}4p_y^{0.04}3d_{x^2-y^2}^{1.49}3d_{xy}^{1.49}$ $2s^{1.76}2p_z^{1.12}2p_x^{0.60}2p_y^{0.60}$	Co(a^4F; M=±3) C(^{3}P; M=∓1) $1^2\Delta$	±2, 0
$2^4\Phi$	$0.58\left\|\left(1\sigma^2 2\sigma^2 3\sigma^1\right)\left(1\pi_x^2 1\pi_y^2 2\pi_y^1 1\delta_+^2 1\delta_-^1 - 1\pi_x^2 2\pi_x^1 1\pi_y^2 1\delta_+^1 1\delta_-^2\right)\right\rangle_{B_1}$	$4s^{0.92}4p_z^{0.22}3d_{z^2}^{1.37}3d_{xz}^{1.55}4p_x^{0.07}3d_{yz}^{1.55}4p_y^{0.07}3d_{x^2-y^2}^{1.49}3d_{xy}^{1.49}$ $2s^{1.73}2p_z^{0.71}2p_x^{0.86}2p_y^{0.86}$	Co(b^4F; M=±3) C(^{3}P; M=0) $2^4\Phi$	±3, 0
$3^4\Pi$	$0.59\left\|\left(1\sigma^2 2\sigma^2 3\sigma^1\right)\right.$ $\left.\left(1\pi_x^2 1\pi_y^2 2\pi_y^1 1\delta_+^2 1\delta_-^1 + 1\pi_x^2 2\pi_x^1 1\pi_y^2 1\delta_+^1 1\delta_-^2\right)\right\rangle_{B_1}$	$4s^{0.91}4p_z^{0.22}3d_{z^2}^{1.39}3d_{xz}^{1.55}4p_x^{0.07}3d_{yz}^{1.55}4p_y^{0.07}3d_{x^2-y^2}^{1.49}3d_{xy}^{1.49}$ $2s^{1.73}2p_z^{0.71}2p_x^{0.85}2p_y^{0.85}$	Co(b^4F; M=±1) C(^{3}P; M=0) $3^4\Pi$	±2, ∓1
$4^2\Phi$	$\left\|\left(1\sigma^2 2\sigma^2 3\sigma^1\right)\left[0.51\left(1\pi_x^2 2\bar{\pi}_x^1 1\pi_y^2 1\delta_+^1 1\delta_-^2\right)-\right.\right.$ $-0.42\left(1\pi_x^2 1\pi_y^2 2\bar{\pi}_y^1 1\delta_+^2 1\delta_-^1\right)+$ $+0.28\left(1\pi_x^2 1\pi_y^2 2\pi_y^1 1\delta_+^2 1\bar{\delta}_-^1\right)+$ $\left.\left.+0.22\left(1\pi_x^2 2\bar{\pi}_x^1 1\pi_y^2 2\bar{\pi}_y^1 1\delta_+^2 1\delta_-^2\right)\right]\right\rangle_{B_1}$	$4s^{0.95}4p_z^{0.28}3d_{z^2}^{1.21}3d_{xz}^{1.59}4p_x^{0.04}3d_{yz}^{1.59}4p_y^{0.04}3d_{x^2-y^2}^{1.49}3d_{xy}^{1.49}$ $2s^{1.74}2p_z^{0.78}2p_x^{0.85}2p_y^{0.85}$	Co(^{4}F; M=±3) C(^{3}P; M=0) $4^2\Phi$	±3, 0
$5^2\Phi$	$\left\|0.54\left(1\sigma^2 2\sigma^2 3\bar{\sigma}^1 1\pi_x^2 2\pi_x^1 1\pi_y^2 1\delta_+^1 1\delta_-^2\right)+\right.$ $+0.41\left(1\sigma^2 2\sigma^2 3\sigma^1 1\pi_x^2 1\pi_y^2 2\pi_y^1 1\delta_+^2 1\bar{\delta}_-^1\right)+$ $+0.36\left(1\sigma^2 2\sigma^2 3\sigma^1 1\pi_x^2 1\pi_y^2 2\bar{\pi}_y^1 1\delta_+^2 1\delta_-^1\right)$ $\left.-0.19\left(1\sigma^2 2\sigma^2 3\sigma^1 1\bar{\pi}_x^2 2\pi_x^1 1\pi_y^2 2\pi_y^1 1\delta_+^2 1\bar{\delta}_-^1\right)\right\rangle_{B_1}$	$4s^{0.99}4p_z^{0.22}3d_{z^2}^{1.37}3d_{xz}^{1.55}4p_x^{0.05}3d_{yz}^{1.55}4p_y^{0.05}3d_{x^2-y^2}^{1.49}3d_{xy}^{1.49}$ $2s^{1.69}2p_z^{0.68}2p_x^{0.88}2p_y^{0.88}$	Co(^{4}F; M=±3) C(^{3}P; M=0) $5^2\Phi$	±2, ±1

Electronic Structure of Cobalt Carbide

J. Phys. Chem. A, Vol. 110, No. 28, 2006 **8959**

TABLE 3: (Continued)
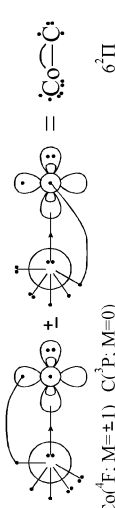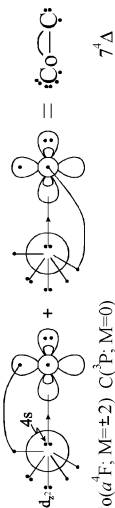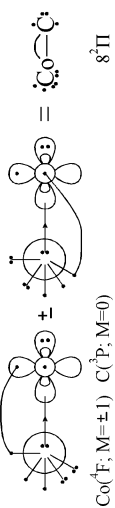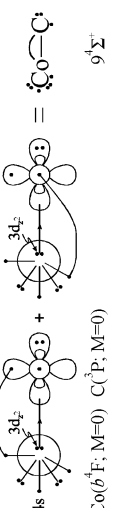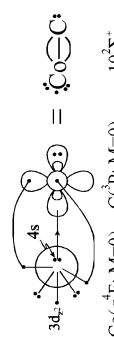
State	Leading Configurations	Population Analysis	vbL	M, M
$6^2\Pi$	$\big\|\sigma^2 2\sigma^2 3\sigma^1\rangle\big[0.43\|1\pi_x^2 2\overline{\pi}_x^1 1\pi_y^2 1\delta_+^1 1\delta_-^2\rangle +$ $+ 0.40\|1\pi_x^2 1\pi_y^2 2\overline{\pi}_y^1 1\delta_+^2 1\delta_-^1\rangle + 0.21(\|1\pi_x^2 2\overline{\pi}_x^1$ $1\pi_y^1 2\overline{\pi}_y^1 1\delta_+^1 1\delta_-^2\rangle + 0.19\|1\pi_x^1 2\overline{\pi}_x^1 1\pi_y^2 2\overline{\pi}_y^1 1\delta_+^2 1\delta_-^1\rangle) +$ $+ 0.18\|1\pi_x^1 2\overline{\pi}_x^1 1\pi_y^2 2\pi_y^1 1\delta_+^2 1\overline{\delta}_-^1\rangle\big]+$ $+ 0.22\|\sigma^2 2\sigma^2 3\sigma^1 1\pi_x^2 1\pi_y^2 2\overline{\pi}_y^1 1\delta_+^1 1\delta_-^1\rangle\big\rangle_{B_1}$	$4s^{1.00} 4p_z^{0.29} 3d_{z^2}^{1.28} 3d_{xz}^{1.60} 4p_x^{0.04} 3d_{yz}^{1.60} 4p_y^{0.04} 3d_{x^2-y^2}^{1.41} 3d_{xy}^{1.41}$ $2s^{1.74} 2p_z^{0.82} 2p_x^{0.85} 2p_y^{0.85}$	 Co(^{4}F; M=±1) C(^{3}P, M=0) $6^2\Pi$	±1, 0
$7^4\Delta$	$\big\|\sigma^2 2\sigma^2 3\sigma^1\rangle\big[0.43\|1\pi_x^2 1\pi_y^1 2\pi_y^1 + 1\pi_x^1 2\pi_x^1 1\pi_y^2\rangle$ $- 0.18(2\pi_x^2 1\pi_y^1 2\pi_y^1 + 1\pi_x^1 2\pi_x^1 2\pi_y^2)\|1\delta_+^1 1\delta_-^2\rangle +$ $+ 0.40\|\sigma^2 2\sigma^2 3\sigma^1 4\sigma^1 1\pi_x^2 1\pi_y^2 1\delta_+^1 1\delta_-^2\rangle\big\rangle_{A_1}$	$4s^{1.13} 4p_z^{0.33} 3d_{z^2}^{1.87} 3d_{xz}^{1.14} 4p_x^{0.05} 3d_{yz}^{1.14} 4p_y^{0.05} 3d_{x^2-y^2}^{1.00} 3d_{xy}^{2.00}$ $2s^{1.73} 2p_z^{0.88} 2p_x^{0.81} 2p_y^{0.81}$	 Co(a^4F; M=±2) C(^{3}P; M=0) $7^4\Delta$	±2, 0
$8^2\Pi$	$\big[0.53\|\sigma^2 2\sigma^2 3\sigma^1 1\pi_x^2 1\pi_y^2 2\pi_y^1 1\delta_+^2 1\overline{\delta}_-^1\rangle$ $- 0.52\|\sigma^2 2\sigma^2 3\overline{\sigma}^1 1\pi_x^2 2\pi_x^1 1\pi_y^2 1\delta_+^1 1\delta_-^2\rangle$ $- 0.17\big(\|\sigma^2 2\sigma^2 3\sigma^1 1\pi_x^2 2\overline{\pi}_x^1 1\pi_y^2 1\delta_+^1 1\delta_-^2\rangle\big)\big\rangle_{B_1}$	$4s^{0.99} 4p_z^{0.21} 3d_{z^2}^{1.37} 3d_{xz}^{1.57} 4p_x^{0.06} 3d_{yz}^{1.57} 4p_y^{0.06} 3d_{x^2-y^2}^{1.49} 3d_{xy}^{1.49}$ $2s^{1.70} 2p_z^{0.71} 2p_x^{0.86} 2p_y^{0.86}$	 Co(^{4}F; M=±1) C(^{3}P; M=0) $8^2\Pi$	±2, ∓1
$9^4\Sigma^+$	$\big\|\sigma^2 2\sigma^2 3\sigma^1\rangle\big[0.37\|1\pi_x^2 1\pi_y^1 2\pi_y^1 + 1\pi_x^1 2\pi_x^1 1\pi_y^2\rangle$ $+ 0.23(\|1\pi_x^1 2\overline{\pi}_x^1 1\pi_y^1 2\pi_y^1\rangle + 0.19\|1\pi_x^1 2\pi_x^1 1\pi_y^1 2\overline{\pi}_y^1\rangle\big]$ $1\delta_+^2 1\delta_-^2 + (\|\sigma^2 2\sigma^2 3\sigma^1\rangle\big[0.30\|1\pi_x^2 2\overline{\pi}_x^1 1\pi_y^2 2\pi_y^1\rangle$ $+ 0.22\|1\pi_x^2 2\pi_x^1 1\pi_y^2 2\overline{\pi}_y^1\rangle\big]1\delta_+^1 1\delta_-^1$ $- 0.20\|1\pi_x^2 2\pi_x^1 1\pi_y^2 2\pi_y^1 1\delta_+^1 1\overline{\delta}_-^1\rangle\}$ $+ 0.20\|\sigma^2 2\sigma^2 3\sigma^1 4\sigma^1 1\pi_x^2 1\pi_y^2 1\delta_+^2 1\delta_-^2\rangle\big\rangle_{A_1}$	$4s^{0.97} 4p_z^{0.30} 3d_{z^2}^{1.20} 3d_{xz}^{1.39} 4p_x^{0.05} 3d_{yz}^{1.39} 4p_y^{0.05} 3d_{x^2-y^2}^{1.00} 3d_{xy}^{1.65}$ $2s^{1.72} 2p_z^{0.78} 2p_x^{0.88} 2p_y^{0.88}$	 Co(b^4F; M=0) C(^{3}P; M=0) $9^4\Sigma^+$	0, 0
$10^2\Sigma^+$	$\big[0.31(\|\sigma^2 2\sigma^2 3\sigma^2\rangle - 0.25(\|\sigma^2 2\sigma^2 3\overline{\sigma}^1 4\sigma^1\rangle\big]$ $(1\pi_x^2 1\pi_y^2 1\delta_+^1 1\delta_-^2) + (\|\sigma^2 2\sigma^2 3\sigma^1\rangle\big[0.30(\|\pi_x^2 2\pi_x^1 1\pi_y^2\rangle +$ $+ 1\pi_x^2 1\overline{\pi}_x^1 2\pi_y^1) - 0.29(\|\pi_x^2 1\pi_y^2\rangle\big]1\delta_+^1 1\delta_-^2$ $- 0.19\|\sigma^2 2\sigma^2 3\overline{\sigma}^1 1\pi_x^2 2\pi_x^1 1\pi_y^2 1\delta_+^2 1\delta_-^1\rangle\big\rangle_{A_1}$	$4s^{1.06} 4p_z^{0.23} 3d_{z^2}^{1.23} 3d_{xz}^{1.29} 4p_x^{0.04} 3d_{yz}^{1.29} 4p_y^{0.04} 3d_{x^2-y^2}^{1.79} 3d_{xy}^{1.79}$ $2s^{1.67} 2p_z^{0.78} 2p_x^{0.86} 2p_y^{0.86}$	 Co(a^4F; M=0) C(^{3}P; M=0) $10^2\Sigma^+$	±1, ∓1

TABLE 3: (Continued)
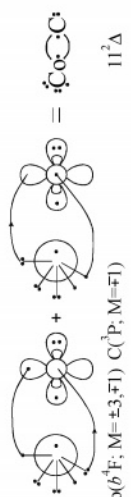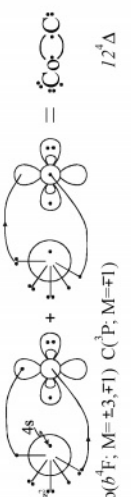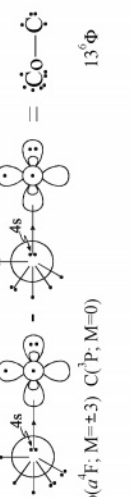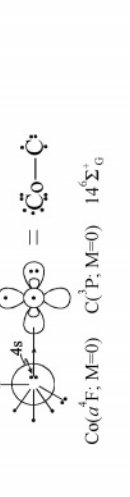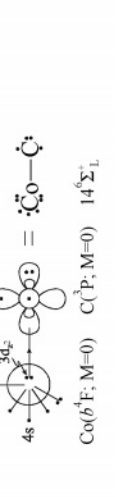
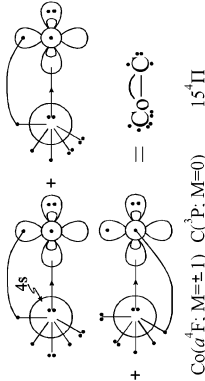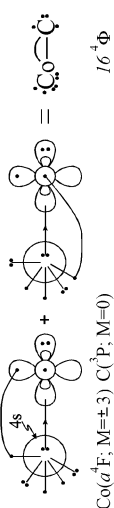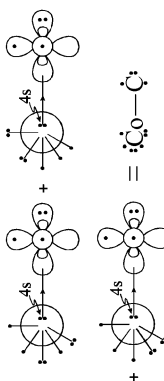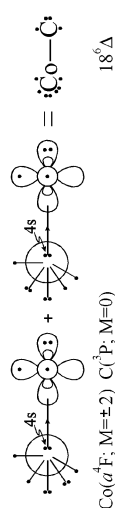| State	Leading Configurations	Population Analysis	vbL	M, M
$11^2\Delta$	$\|1\sigma^2 2\sigma^2 3\sigma^1 4\sigma^1 [0.64(\|\pi_x^2 1\pi_y^2) - 0.19(\|\pi_x^2 2\pi_y^2 + 2\pi_x^1\|\pi_y^2)](\|\bar\delta_+^1 1\delta_-^2) + 0.36(\|\sigma^2 2\sigma^2 3\sigma^1 4\sigma^1 1\pi_x^2 1\pi_y^2 1\delta_+^1 1\delta_-^2) - 0.18(\|\sigma^2 2\sigma^2 3\sigma^1 4\sigma^1 (\|\pi_x^1\|\bar\pi_y^1 2\bar\pi_y^1 + 1\bar\pi_x^1 2\bar\pi_x^1 1\pi_y^2)(\|\delta_+^1 1\delta_-^2)\rangle_{A_1}$	$4s^{1.05} 4p_z^{0.38} 3d_{z^2}^{1.82} 3d_{xz}^{1.25} 4p_x^{0.04} 3d_{yz}^{1.25} 4p_y^{0.04} 3d_{x^2-y^2}^{1.50} 3d_{xy}^{1.50}$ $2s^{1.69} 2p_z^{1.00} 2p_x^{0.71} 2p_y^{0.71}$	Co(b^4F; M=±3,∓1) C(^{3}P; M=∓1) $11^2\Delta$	±3, ∓1
$12^4\Delta$	$0.50\|\sigma^2 2\sigma^2 3\sigma^1 4\sigma^1 1\pi_x^2 1\pi_y^2 1\delta_+^2 1\delta_-^1\| - 0.38\|\sigma^2 2\sigma^2 3\sigma^2 (1\pi_x^1 2\pi_x^1 1\pi_y^2 + 1\pi_x^2 1\pi_y^1 2\pi_y^1)(1\delta_+^2 1\delta_-^1)\rangle_{A_1}$	$4s^{1.14} 4p_z^{0.33} 3d_{z^2}^{1.68} 3d_{xz}^{1.26} 4p_x^{0.04} 3d_{yz}^{1.26} 4p_y^{0.04} 3d_{x^2-y^2}^{1.98} 3d_{xy}^{1.01}$ $2s^{1.74} 2p_z^{1.05} 2p_x^{0.70} 2p_y^{0.70}$	Co(a^4F; M=±3,∓1) C(^{3}P; M=∓1) $12^4\Delta$	±1, ±1
$13^6\Phi$	$\|0.45(\|\sigma^2 2\sigma^2 3\sigma^1 \|\pi_x^2 2\pi_x^1 1\pi_y^1 2\pi_y^1 1\delta_+^1 1\delta_-^2 - 1\pi_x^1 2\pi_x^1 1\pi_y^2 1\delta_+^2 1\delta_-^1) - (\|\sigma^2 2\sigma^2 3\sigma^1 4\sigma^1 \{[0.25(\|\pi_x^1 2\bar\pi_x^1 1\pi_y^2 2\pi_y^1) + 0.19(\|\pi_x^1 2\pi_x^1 1\pi_y^2 2\bar\pi_y^1)] (1\delta_+^2 1\delta_-^1) - [0.24(\|\pi_x^2 2\bar\pi_x^1 1\pi_y^1 2\pi_y^1) + 0.24(\|\pi_x^2 2\pi_x^1 1\pi_y^1 2\bar\pi_y^1)](1\delta_+^1 1\delta_-^2)\} + 0.18(\|\sigma^2 3\sigma^1 4\sigma^2 (1\pi_x^1 2\pi_x^1 1\pi_y^2 1\delta_+^2 1\delta_-^1 - 1\pi_x^2 2\pi_x^1 1\pi_y^1 2\pi_y^1 1\delta_+^1 1\delta_-^2)\rangle_{B_1}$	$4s^{1.03} 4p_z^{0.33} 3d_{z^2}^{1.09} 3d_{xz}^{1.51} 4p_x^{0.05} 3d_{yz}^{1.51} 4p_y^{0.05} 3d_{x^2-y^2}^{1.49} 3d_{xy}^{1.49}$ $2s^{1.71} 2p_z^{0.80} 2p_x^{0.92} 2p_y^{0.92}$	Co(a^4F; M=±3) C(^{3}P; M=0) $13^6\Phi$	±3, 0
$14^6\Sigma_G^+$	$\|[0.63(\|\sigma^2 2\sigma^2 3\sigma^1) - 0.25(\|\sigma^2 3\sigma^1 4\sigma^2)] (1\pi_x^2 2\pi_x^1 1\pi_y^2 2\pi_y^1 1\delta_+^1 1\delta_-^1) + 0.33(\|\sigma^2 2\sigma^2 3\sigma^1 1\pi_x^1 2\pi_x^1 1\pi_y^1 2\pi_y^1 1\delta_+^2 1\delta_-^2) - (\|\pi_x^2 2\pi_x^1 1\pi_y^2 2\pi_y^1 1\delta_+^1 1\delta_-^1)[0.29(\|\pi_x^2 2\bar\pi_x^1 1\pi_y^2 2\pi_y^1 1\delta_+^1 1\delta_-^1) - (\|\pi_x^2 2\pi_x^1 1\pi_y^2 2\bar\pi_y^1 1\delta_+^1 1\delta_-^1)] + 0.24(\|\pi_x^2 2\pi_x^1 1\pi_y^2 2\bar\pi_y^1 1\delta_+^1 1\delta_-^1) + 0.19(\|\pi_x^1 2\pi_x^1 1\pi_y^1 2\pi_y^1 1\delta_+^2 1\delta_-^2 - 1\pi_x^2 2\pi_x^1 1\pi_y^2 2\pi_y^1 1\delta_+^1 1\delta_-^1)\rangle_{A_1}$	$4s^{1.07} 4p_z^{0.31} 3d_{z^2}^{1.07} 3d_{xz}^{1.76} 4p_x^{0.06} 3d_{yz}^{1.76} 4p_y^{0.06} 3d_{x^2-y^2}^{1.24} 3d_{xy}^{1.24}$ $2s^{1.73} 2p_z^{0.78} 2p_x^{0.93} 2p_y^{0.93}$	Co(a^4F; M=0) C(^{3}P; M=0) $14^6\Sigma_G^+$	0, 0
$14^6\Sigma_L^+$	$\|0.80(\|\sigma^2 2\sigma^2 3\sigma^1 2\pi_x^1 1\pi_y^2 2\pi_y^1 1\delta_+^1 1\delta_-^1) + 0.27(\|\sigma^2 2\sigma^2 3\sigma^1 1\pi_x^1 2\pi_x^1 1\pi_y^1 2\pi_y^1 1\delta_+^2 1\delta_-^2) - 0.19(\|\sigma^2 3\sigma^1 4\sigma^2 1\pi_x^2 2\pi_x^1 1\pi_y^2 2\pi_y^1 1\delta_+^1 1\delta_-^1)\rangle_{A_1}$	$4s^{0.95} 4p_z^{0.24} 3d_{z^2}^{1.36} 3d_{xz}^{1.81} 4p_x^{0.13} 3d_{yz}^{1.81} 4p_y^{0.13} 3d_{x^2-y^2}^{1.11} 3d_{xy}^{1.11}$ $2s^{1.71} 2p_z^{0.70} 2p_x^{0.93} 2p_y^{0.93}$	Co(b^4F; M=0) C(^{3}P; M=0) $14^6\Sigma_L^+$	

Electronic Structure of Cobalt Carbide

J. Phys. Chem. A, Vol. 110, No. 28, 2006 **8961**

TABLE 3: (Continued)

State	Leading Configurations	Population Analysis	vbL	M, M
15 $^4\Pi$	$\|0.39(\|\sigma^2 2\sigma^2 3\sigma^2 1\pi_x^2 1\pi_y^2 2\pi_y^1 1\delta_+^1 1\delta_-^1\|$ $+ [0.25(\|\sigma^2 2\sigma^1 3\sigma^2) + 0.23(\|\sigma^2 2\sigma^2 3\sigma^1)$ $(1\pi_x^2 1\pi_y^2 2\pi_y^1 1\delta_+^2 1\delta_-^1 + 1\pi_x^2 2\pi_x^1 1\pi_y^2 1\delta_+^1 1\delta_-^2)\|\rangle_{B_1}$	$4s^{1.14} 4p_z^{0.23} 3d_{z^2}^{1.45} 3d_{xz}^{1.56} 4p_x^{0.06} 3d_{yz}^{1.34} 3d_{x^2-y^2}^{1.34} 3d_{xy}^{1.34}$ $2s^{1.69} 2p_z^{0.78} 2p_x^{0.88} 2p_y^{0.88}$	$= \ddot{C}o{-}\dot{\ddot{C}}$ 15 $^4\Pi$ Co(a^4F; M=±1) C(^{3}P; M=0)	±1, 0
16 $^4\Phi$	$\|0.30(\|\sigma^2 2\sigma^1 3\sigma^2)(\|\pi_x^2 1\pi_y^2 2\pi_y^1 1\delta_+^1 1\delta_-^1 +$ $1\pi_x^2 2\pi_x^1 1\pi_y^2 1\delta_+^1 1\delta_-^2) -$ $0.26(\|\sigma^2 2\sigma^2 3\overline{\sigma}^1 1\pi_x^2 2\pi_x^1 1\pi_y^1 2\pi_y^1 1\delta_+^1 1\delta_-^2) -$ $0.26(\|\sigma^2 2\sigma^2 3\sigma^1 1\overline{\pi}_x^1 2\pi_x^1 1\pi_y^2 2\pi_y^1 1\delta_+^1 1\delta_-^1) -$ $0.20(\|\sigma^2 2\sigma^1 3\sigma^1 4\overline{\sigma}^1 1\pi_x^2 2\pi_x^1 1\pi_y^2 1\delta_+^1 1\delta_-^2) -$ $0.18(\|\sigma^2 2\sigma^1 3\sigma^2 1\pi_x^1 2\pi_x^1 1\pi_y^2 2\pi_y^1 1\delta_+^2 1\delta_-^1)\|\rangle_{B_1}$	$4s^{1.10} 4p_z^{0.24} 3d_{z^2}^{1.20} 3d_{xz}^{1.53} 4p_x^{0.05} 3d_{yz}^{1.53} 4p_y^{0.05} 3d_{x^2-y^2}^{1.49} 3d_{xy}^{1.49}$ $2s^{1.65} 2p_z^{0.77} 2p_x^{0.91} 2p_y^{0.93}$	$= \dot{\ddot{C}}o{-}\dot{\ddot{C}}$ 16 $^4\Phi$ Co(a^4F; M=±3) C(^{3}P; M=0)	±2, ±1
17 $^6\Pi$	$\|0.37(\|\sigma^2 2\sigma^2 3\sigma^1 1\pi_x^2 2\pi_x^1 1\pi_y^2 2\pi_y^1 1\delta_+^1 1\delta_-^1)$ $+ 0.20(\|\sigma^2 2\sigma^1 3\sigma^2 4\sigma^1 1\pi_x^1 2\pi_x^1 1\overline{\pi}_y^1 2\pi_y^1 1\delta_+^1 1\delta_-^1)$ $- 0.34(\|\sigma^2 2\sigma^2 3\sigma^1)(\|\pi_x^2 2\pi_x^1 1\pi_y^1 2\pi_y^1 1\delta_+^1 1\delta_-^2 +$ $1\pi_x^1 2\pi_x^1 1\pi_y^2 2\pi_y^1 1\delta_+^2 1\delta_-^1) - (\|\sigma^2 2\sigma^1 3\sigma^1 4\sigma^1$ $[0.20(\|\pi_x^2 2\overline{\pi}_x^1 1\pi_y^1 2\pi_y^1 + 1\pi_x^1 2\pi_x^1 1\pi_y^1 2\overline{\pi}_y^1)1\delta_+^1 1\delta_-^2 +$ $+ 0.23(\|\pi_x^1 2\overline{\pi}_x^1 1\pi_y^2 2\pi_y^1 1\delta_+^2 1\delta_-^1)]+$ $+ 0.19(\|\sigma^2 2\sigma^1 3\sigma^2)(\|\pi_x^2 2\pi_x^1 1\pi_y^1 2\pi_y^1 1\delta_+^1 1\delta_-^2 -$ $1\pi_x^1 2\pi_x^1 1\pi_y^2 2\pi_y^1 1\delta_+^1 1\delta_-^1)\|\rangle_{B_1}$	$4s^{1.08} 4p_z^{0.32} 3d_{z^2}^{1.34} 3d_{xz}^{1.37} 4p_x^{0.05} 3d_{yz}^{1.66} 4p_y^{0.05} 3d_{x^2-y^2}^{1.34} 3d_{xy}^{1.34}$ $2s^{1.72} 2p_z^{0.79} 2p_x^{0.92} 2p_y^{0.92}$	$= \dot{\ddot{C}}o{-}\dot{\ddot{C}}$ 17 $^6\Pi$ Co(a^4F; M=±1) C(^{3}P; M=0)	±1, 0
18 $^6\Delta$	$\|[0.60(\|\sigma^2 2\sigma^2 3\sigma^2) - 0.26(\|\sigma^2 2\sigma^2 4\sigma^2)]$ $(1\pi_x^1 2\pi_x^1 1\pi_y^1 2\pi_y^1 1\delta_+^1 1\delta_-^2) + (\|\sigma^2 2\sigma^2 3\sigma^1 4\sigma^1)$ $[0.40(\|\pi_x^1 2\pi_x^1 2\pi_y^1 + 1\pi_x^1 2\pi_x^1 1\pi_y^1)$ $- 0.23(\|\pi_x^1 2\pi_x^1 2\pi_y^1 + 2\pi_x^2 1\pi_y^1 2\pi_y^1)]\|1\delta_+^1 1\delta_-^2$ $- 0.23(\|\pi_x^1 2\pi_x^1 1\pi_y^1 2\pi_y^1 1\overline{\delta}_+^1 1\delta_-^2)\|\rangle_{A_1}$	$4s^{1.11} 4p_z^{0.34} 3d_{z^2}^{1.95} 3d_{xz}^{1.04} 4p_x^{0.05} 3d_{yz}^{1.04} 4p_y^{0.05} 3d_{x^2-y^2}^{1.00} 3d_{xy}^{1.99}$ $2s^{1.73} 2p_z^{0.81} 2p_x^{0.91} 2p_y^{0.91}$	$= \ddot{C}o{-}\dot{\ddot{C}}$ 18 $^6\Delta$ Co(a^4F; M=±2) C(^{3}P; M=0)	±2, 0

9 $^4\Sigma^+$. This is a double bonded (σ, π) quartet located 41.7 (42.3) kcal/mol above the X state at the MRCI(+Q) level, showing also strongly multireference character.

C. Sextets: 13 $^6\Phi$, 14 $^6\Sigma^+$, 17 $^6\Pi$, and 18 $^6\Delta$. All four sextets above display strong multireference character, they are σ-single bonded and the in situ carbon atom finds itself in the $M = 0$ component of its ^3P state. In all cases the σ-bond is formed by the transfer of about 0.5 e$^-$ from the 4s^2 Co distribution to the empty 2p$_z$ orbital of the C atom. These four sextets lie within an energy range of 5 kcal/mol, reflecting their similar bonding interaction (Figure 5).

The PEC of the 14 $^6\Sigma^+$ shows a global (G) and a local (L) minimum, the result of an avoided crossing with another (not calculated) $^6\Sigma^+$ state correlating to Co(b^{4}F; $M = 0$) + C(^{3}P; $M = 0$). The barrier height between the G$-$L minima is 2.34 kcal/mol measured from the G-minimum; Figure 5.

4. Summary and Final Remarks

Employing mainly multireference variational methods (MRCI) combined with quantitative basis sets, we calculated 19 states (8 doublets, 7 quartets, 4 sextets) of the diatomic carbide CoC, spanning an energy range of 2.2 eV. For all states we report full potential energy curves, energetics, the usual spectroscopic parameters, dipole moments calculated as expectation values ($\langle u \rangle$) and also by the finite field method (μ_{FF}), and spin$-$orbit (SO) splittings for the eight lowest states other than states of Σ symmetry. With the exception of the two lower states the generally contracted basis set [7s6p4d3f2g$_{Co}$ 5s4p3d2f1g$_C$] was used; for the X $^2\Sigma^+$ and 1 $^2\Delta$ states the quadruple-ζ cc-basis set for the Co atom was also employed. In addition, for these two states only, RCCSD(T) calculations have been performed around the equilibrium geometry, whereas semicore correlation effects (3s^{2}3p^6 of Co) and scalar relativistic corrections have been taken into account. A summary of our main results follows.

(i) It seems almost certain that the ground state is of $^2\Sigma^+$ symmetry, with a $^2\Delta$ state lying higher by less than 3 kcal/mol. Our best estimate of its $D_e(D_0)$ value is 83(82) kcal/mol at $r_e = 1.541$ Å, 0.02 Å shorter than the experimental bond length. The calculated $^2\Delta_{5/2} - {^2\Delta_{3/2}}$ splitting is 989 cm^{-1} at the MRCI level in good agreement with the experimental one of 952 cm^{-1}.

(ii) All 19 calculated states correlate adiabatically to the ground-state atoms Co(a^{4}F) + C(^{3}P) and are bound, with binding energies (D_e) ranging from 84.2 (X $^2\Sigma^+$) to 29.4 kcal/mol (18 $^6\Delta$) at the MRCI+Q level. The ground state has the shortest bond length of all calculated states with the largest bond length being 2.003 Å (18 $^6\Delta$).

(iii) The doublets are double or triple bonded, the quartets double bonded, and the sextets single bonded. With the exception of the 1 $^2\Delta$, 11 $^2\Delta$, and 12 $^4\Delta$ states, where the in situ C(^{3}P) atom interacts with its $M = \pm 1$ component, in the remaining 16 states it finds itself in the $M = 0$ projection. On the other hand, d$_{x^2-y^2}(\delta_+)$ and d$_{xy}(\delta_-)$ electrons do not seem to play any significant role in the binding, being localized on the Co atom. In addition, in all states the metal appears to be Mulliken positively charged with a metal-to-carbon charge transfer of about 0.1 to 0.5 e$^-$ depending on the state.

(iv) In accord to previous observations,[1g] finite field electric dipole moments (μ_{FF}) are significantly larger than expectation value ones ($\langle u \rangle$), by as much as 1 Debye (X $^2\Sigma^+$). We believe that, in general, μ_{FF} values should be trusted more than $\langle u \rangle$ ones; therefore, the dipole moment of the CoC X $^2\Sigma^+$ state must be pretty close to 2.0 D.

(v) The T_e's of the following pairs or groups differ by about 1 mhartree at the MRCI level and obviously their real ordering is probably different, {6 $^2\Pi$, 7 $^4\Delta$}, {10 $^2\Sigma^+$, 11 $^2\Delta$, 12 $^4\Delta$, 13 $^6\Phi$}, {14 $^6\Sigma^+$, 15 $^4\Pi$, 16 $^4\Phi$}, {17 $^6\Pi$, 18 $^6\Delta$}. The ordering is reversed by adding the zero point energy correction $\Delta\omega_e/2$, only for the pair {12 $^4\Delta$, 13 $^6\Phi$}.

References and Notes

(1) (a) Kalemos, A.; Mavridis, A.; Harrison, J. F. *J. Phys. Chem. A* **2001**, *105*, 755. (b) Kalemos, A.; Mavridis, A. *J. Phys. Chem. A* **2002**, *106*, 3905. (c) Kalemos, A.; Dunning, T. H., Jr.; Mavridis, A. *J. Chem. Phys.* **2005**, *123*, 014301. (d) Kalemos, A.; Dunning, T. H., Jr.; Mavridis, A. *J. Chem. Phys.* **2005**, *123*, 014302. (e) Kalemos, A.; Dunning, T. H., Jr.; Mavridis, A. In press. (f) Tzeli, D.; Mavridis, A. *J. Chem. Phys.* **2002**, *116*, 4901. (g) Tzeli, D.; Mavridis, A. *J. Chem. Phys.* **2003**, *118*, 4984; **2005**, *122*, 056101.

(2) Harrison, J. F. *Chem. Rev.* **2000**, *100*, 679 and references therein.

(3) van Zee, R. J.; Bianchini, J. J.; Weltner, W., Jr. *Chem. Phys. Lett.* **1986**, *127*, 314.

(4) Barnes, M.; Merer, A. J.; Metha, G. F. *J. Chem. Phys.* **1995**, *103*, 8360.

(5) Adam, A. G.; Peers, J. R. D. *J. Mol. Spectrosc.* **1997**, *181*, 24.

(6) Brewster, M. A.; Ziurys, L. M. *Astrophys. J.* **2001**, *559*, L163.

(7) Gutsev, G. L.; Andrews, L.; Bauschlicher, C. W., Jr. *Theor. Chem. Acc.* **2003**, *109*, 298.

(8) Borin, A. C.; Gobbo, J. P.; Roos, B. O. *Chem. Phys. Lett.* **2006**, *418*, 311.

(9) Finley, J.; Malmqvist, P.-Å.; Roos, B. O.; Serrano-Andrés, L. *Chem. Phys. Lett.* **1998**, *288*, 299.

(10) Roos, B. O.; Lindh, R.; Malmqvist, P.-Å.; Veryazov, V.; Widmark, P.-O. *J. Phys. Chem. A* **2005**, *109*, 6575 and references therein.

(11) Bauschlicher, C. W., Jr. *Theor. Chim. Acta* **1995**, *92*, 183.

(12) Dunning, T. H., Jr. *J. Chem. Phys.* **1989**, *90*, 1007.

(13) Balabanov, N. B.; Peterson, K. A. *J. Chem. Phys.* **2005**, *123*, 064107.

(14) Werner, H.-J.; Knowles, P. J. *J. Chem. Phys.* **1988**, *89*, 5803. Knowles, P. J.; Werner, H.-J. *Chem. Phys. Lett.* **1988**, *145*, 514. Werner, H.-J.; Reinsch, E. A. *J. Chem. Phys.* **1982**, *76*, 3144; Werner, H.-J. *Adv. Chem. Phys.* **1987**, *LXIX*, 1.

(15) Douglas, M.; Kroll, N. M. *Ann. Phys. N. Y.* **1974**, *82*, 89. Hess, B. A. *Phys. Rev. A* **1985**, *32*, 756. Hess, B. A. *Phys. Rev. A* **1986**, *33*, 3742. Jansen, G.; Hess, B. A. *Phys. Rev. A* **1989**, *39*, 6016.

(16) Berning, A.; Schweizer, M.; Werner, H.-J.; Knowles, P. J.; Palmieri, P. *Mol. Phys.* **2000**, *98*, 1823.

(17) Boys, S. F.; Bernardi, F. *Mol. Phys.* **1970**, *19*, 553. Liu, B.; Mclean, A. D. *J. Chem. Phys.* **1973**, *59*, 4557. Jansen, H. B.; Ros, P. *Chem. Phys. Lett.* **1969**, *3*, 140.

(18) Docken, K.; Hinze, J. *J. Chem. Phys.* **1972**, *57*, 4928. Werner, H.-J.; Meyer, W. *J. Chem. Phys.* **1981**, *74*, 5794.

(19) Langhoff, S. R.; Davidson, E. R. *Int. J. Quantum Chem.* **1974**, *8*, 61; Blomberg, M. R. A.; Sieghbahm, P. E. M. *J. Chem. Phys.* **1983**, *78*, 5682.

(20) MOLPRO 2002 is a package of ab initio programs written by Werner, H.-J.; Knowles, P. J. with contributions by Amos, R. D.; Bernhardsson, A.; Berning, A.; Celani, P.; Cooper, D. L.; Deegan, M. J. O.; Dobbyn, A. J.; Eckert, F.; Hampel, C.; Hetzer, G.; Korona, T.; Lindh, R.; Lloyd, A. W.; McNikolas, S. J.; Manby, F. R.; Meyer, W.; Mura, M. E.; Nicklass, A.; Palmieri, P.; Pitzer, R.; Rauhut, G.; Schütz, M.; Schumann, U.; Stoll, H.; Stone, A. J.; Tarroni, R.; Thorsteinsson, T.

(21) Moore, C. E. *Atomic Energy Levels*; NSRDS-NBS Circular No. 35; NBS: Washington, DC, 1971.

(22) Tzeli, D.; Mavridis, A. Unpublished results.

(23) Gupta, S. K.; Gingerich, K. A. *J. Chem. Phys.* **1981**, *74*, 3584.

(24) Brugh, D. J.; Morse, M. D. *J. Chem. Phys.* **1997**, *107*, 9772.

(25) Brugh, D. J.; Morse, M. D. *J. Chem. Phys.* **2002**, *117*, 10703.